

Numerical investigation of design and operating parameters on CHI spheromak performance

J.B. O'Bryan, C.A. Romero-Talamás
(University of Maryland, Baltimore County)

S. Woodruff, J.E. Stuber, C. Bowman, P.E. Sieck
(Woodruff Scientific, Inc.)

2016 US-Japan CT Workshop
August 24, 2016

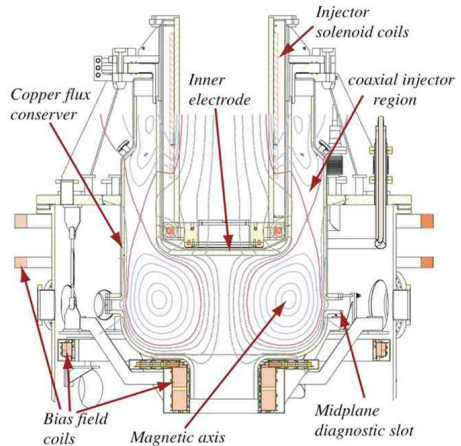


This work is supported by the Defense Advanced Research Projects Agency (DARPA) under Grant Number N66001-14-1-4044.

Introduction & Motivation

The CHI spheromak is formed and sustained through driven magnetic self-organization.

- During CHI, two electrodes connected by vacuum magnetic flux are biased relative to each other.
- Current flows along the magnetic field lines, producing an expanding flux bubble that fills the conducting vacuum vessel.
- A current-driven $n_\phi = 1$ magnetic instability changes the magnetic topology.
- For a simply-connected device, this instability is called the “column mode.”

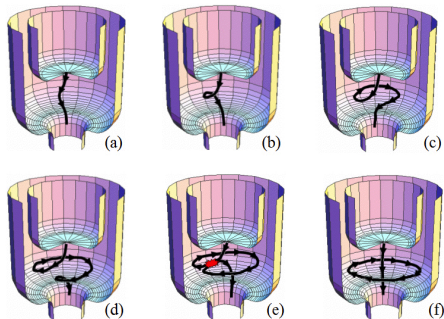


Sustained Spheromak Physics eXperiment (SSPX) Design¹

¹E.B. Hooper et. al. *PPCF*. **54**. 2012.

The column mode is an $n_\phi = 1$ kink instability of the current column near the geometric axis.

- The column mode acts as a (semi-) coherent dynamo that converts toroidal flux into poloidal flux, i.e. predominantly poloidal current into toroidal current.²
- The column mode is self-stabilizing, as the buildup of poloidal flux effectively reduces the value of $\lambda = \mu_0 J_{\parallel} / B$.
- Resistive decay of the core toroidal current increases λ , triggering instability and toroidal current drive.



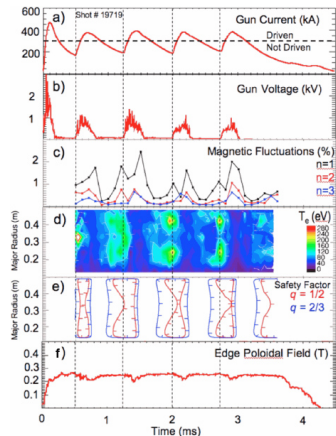
Evolution of the column mode³

²C.R. Sovinec et. al. *Phys. Plas.* **8**. 2001.

³C.A. Romero-Talamás et. al. *Phys. Plas.* **13**. 2006.

SSPX achieved encouraging results, despite being limited by the power driving system and wall heat dissipation.

- The Sustained Spheromak Physics eXperiment (SSPX) achieved $T_e \sim 0.5$ keV, $B_{tor} > 1$ T, $I_p \sim 1$ MA, and peak $\beta_e > 5\%$.
- The power system on SSPX could sustain hundreds of kiloamperes for about 5 ms and was configurable to produce a series of pulses of different amplitudes and durations.
- The wall was a tungsten-coated copper shell, including the injector region, which was subjected to the largest heat loads.



Electron transport during multipulse operation⁴

⁴E.B. Hooper et. al. *PPCF*. **54**. 2012.

The objective of this project is to develop the spheromak concept into a compact, pulsed fusion device for the efficient production of neutrons (and/or electricity).

- Despite its promise as a confinement concept, the spheromak has only been studied at the basic plasma science and concept exploration levels.
- We're exploring two separate approaches (multi-pulse CHI and magnetic flux compression) for sustaining and heating a spheromak plasma to fusion temperatures.
- For both approaches, the initial spheromak plasma is formed by CHI.
- A successful device would achieve high average neutron flux in a relatively compact footprint, e.g. comparable to a few shipping pallets including the power supply.
- This concept is also intended to be used as a platform for developing liquid lithium walls.

This study seeks to explore and optimize the formation of the CHI spheromak and its magnetic compression.

- This presentation focuses on the results of numerical computation with the NIMROD code.
- Analytic scaling relations and engineering design are covered in the presentation by P.E. Sieck.
- This study expands beyond the design and achievable operational regimes of previous experiments (e.g. SSPX) in order to find candidates for future experimental studies.
- At the moment, the formation and compression calculations are separate, but we intend to couple them.

Numerical Model

The computations solve the low-frequency MHD model, starting from vacuum magnetic field and cold fluid.

$$\frac{\partial n}{\partial t} + \nabla \cdot (n\mathbf{v}) = 0$$

$$\rho \left(\frac{\partial \mathbf{v}}{\partial t} + \mathbf{v} \cdot \nabla \mathbf{v} \right) = \mathbf{J} \times \mathbf{B} - \nabla p + \nabla \cdot \underline{\underline{\Pi}}(\mathbf{W}) \quad \text{where } \underline{\underline{\mathbf{W}}} = \nabla \mathbf{v} + \nabla \mathbf{v}^T - (2/3)(\nabla \cdot \mathbf{v})\mathbf{I}$$

$$\frac{2n}{3} \left(\frac{\partial T_e}{\partial t} + \mathbf{v}_e \cdot \nabla T_e \right) = -nT_e \nabla \cdot \mathbf{v}_e - \nabla \cdot \left[\kappa_{\parallel e} \hat{\mathbf{b}}\hat{\mathbf{b}} + \kappa_{\perp e} \mathbf{I} \right] \cdot \nabla T_e + n\sigma (T_i - T_e) + \eta J^2$$

$$\frac{2n}{3} \left(\frac{\partial T_i}{\partial t} + \mathbf{v}_i \cdot \nabla T_i \right) = -nT_i \nabla \cdot \mathbf{v}_i - \nabla \cdot \left[\kappa_{\parallel i} \hat{\mathbf{b}}\hat{\mathbf{b}} + \kappa_{\perp i} \mathbf{I} \right] \cdot \nabla T_i + n\sigma (T_e - T_i)$$

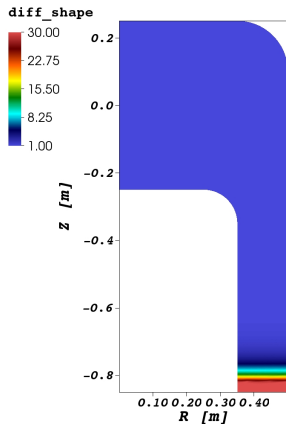
$$\frac{\partial \mathbf{B}}{\partial t} + \nabla \times \left[\eta \mathbf{J} - \mathbf{v} \times \mathbf{B} \right] = 0 \quad \text{where } \mathbf{J} = \mu_0^{-1} \nabla \times \mathbf{B}$$

- The computations use realistic, evolving, locally-computed transport coefficients.
- Our model does not include neutral particle effects (e.g. ionization and recombination).
- The NIMROD code⁵ (nimrodteam.org) is used to solve these systems.

⁵C.R. Sovinec et. al. *J. Comp. Phys.* **195**. 2004.

Only the injector is prescribed: all dynamics follow self-consistently from the model.

- The injector is simulated by specifying $RB_\phi = \mu_0 I_g / 2\pi$ along the injector boundary.
- To encourage the expansion of the flux bubble into the domain, resistivity is enhanced along the injector boundary:
 $\eta \rightarrow \eta + (D_s - 1) \eta_{inj}$.
- The density boundary condition along the injector edge is initially no-flux, but transitions to Dirichlet when $n < n_{crit}$.
- The injector current trace is prescribed, but the injector voltage is produced self-consistently from the plasma model and not an external circuit model.



To consistently model flux compression, the calculations use discrete external field coils.

- The magnetic field from close, discrete compression coils helps stabilize the spheromak to the tilt mode.
- The coils are modeled as a series of single-turn current loops.
- Previous implementations of flux compression in NIMROD have assumed a rectangular (R,Z)-aligned cross-section with uniform B_Z from compression.
- We've generalized the implementation to arbitrarily shaped cross-sections.
- During initialization, B_R , B_Z , and A_ϕ are computed along the edge of the domain for each coil at unit current.

$$B_n(t) = \hat{n} \cdot \sum_{i=1}^{n_{coil}} I_{c,i}(t) \hat{\mathbf{B}}_{c,i}$$

$$B_t(t) = \hat{t} \cdot \mathbf{B}(t)$$

$$E_\phi(t) = - \sum_{i=1}^{n_{coil}} \frac{\partial I_{c,i}}{\partial t} \hat{A}_{\phi,i}$$

$$\mathbf{B}^*(t) = (n_r B_n + t_r B_t) \hat{r} \\ + (n_z B_n + t_z B_t) \hat{z}$$

SSPX multi-pulse

We simulated entire shots in the SSPX spheromak and made direct comparisons between experimental data and synthetic diagnostics.

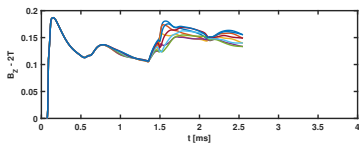
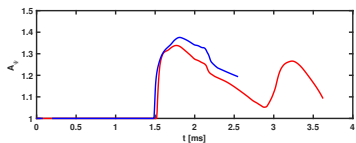
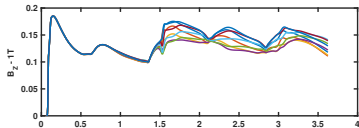
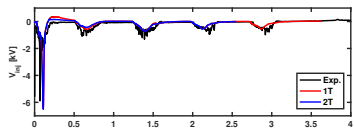
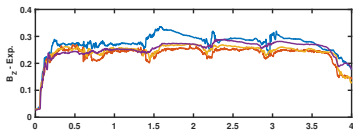
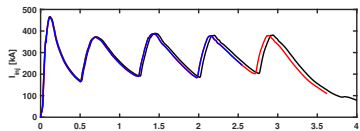
- We determined that a single-temperature resistive MHD model can sufficiently capture relevant physical behavior to qualitatively assess spheromak performance.
- A similar model has been used to study the interaction between thermal transport and magnetic relaxation in previous spheromak studies.^{6 7 8}
- With a simplified physics model, we can explore a greater number of candidate operational modes and flux conserver/injector geometries.
- Once we determine parameters that qualitatively optimize spheromak performance, those cases can be explored with a more complete physics model to quantify the performance gains.

⁶C.R. Sovinec et al. *Phys. Rev. Lett.* 2005.

⁷B.I. Cohen et al. *Phys. Plas.* 2005.

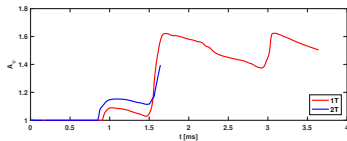
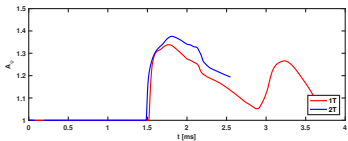
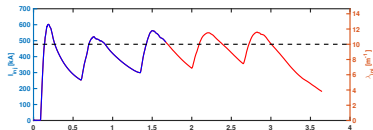
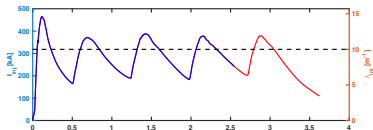
⁸E.B. Hooper et al. *Phys. Plas.* 2008.

For simulations of multi-pulse shots in SSPX, the injector voltage trace and the onset of the column mode agree with the experiment.



SSPX Shot #19719 – 40 mWb bias flux

Shots with similar λ_{inj} traces produce qualitatively different behavior for flux amplification and spheromak lifetime.



Simulated Shot #19719
40 mWb bias flux

Simulated Shot #19766
60 mWb bias flux

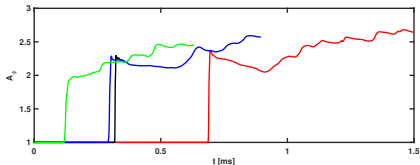
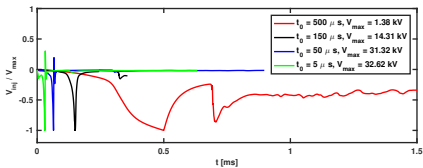
- Linear, ideal MHD stability analysis⁹ predicts the onset of the column mode instability.
- However, it doesn't directly address the accessibility of the equilibria or poloidal flux amplification, which are determined by nonlinear plasma evolution, motivating our formation study.

⁹D.P. Brennan et. al. *Phys. Plas.* **6** (11). 1999.

Formation study

Calculations explore how the rate of change of the injector current affects both spheromak performance and injector voltage requirements.

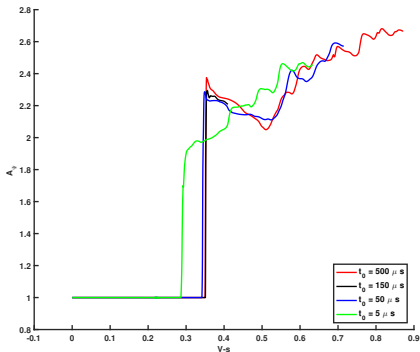
- The voltage requirements of an experiment affect the design and cost of the power supply.
- I_{inj} linearly ramps from 0 to 500 kA over a time t_0 and is then held constant.
- We've found two effective limits for the ramp rate:
 - too slow \rightarrow gradual diffusion, no coherent flux bubble
 - too fast \rightarrow current filaments form along the expanding flux bubble



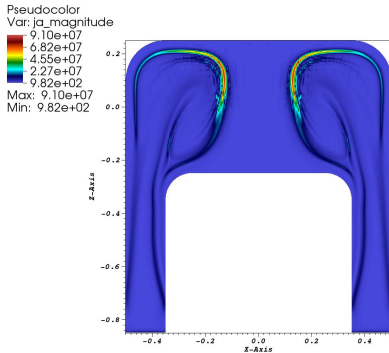
For the initial bias magnetic field, $\tau_A \sim 10^{-5} \text{ s}$.

The column mode onset threshold and poloidal flux amplification (A_Ψ) are largely insensitive to the injector current ramp rate.

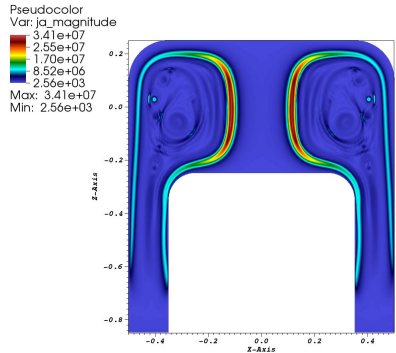
- A_Ψ asymptotes toward a constant value, regardless of the injector current rise time t_0 .
- The poloidal flux amplification produced initially by the column mode ($A_\Psi \approx 2.3$) is much greater than the relative increase later for the same V-s.
- At approximately 0.7 V-s, $A_\Psi \approx 2.5$, or only 9 % more than produced initially.
- We're investigating whether this trend holds during refluxing pulses.



Current filaments along the expanding flux bubble drive MHD activity prior to the column mode.



$t = 2.96814 \times 10^{-5}$ s



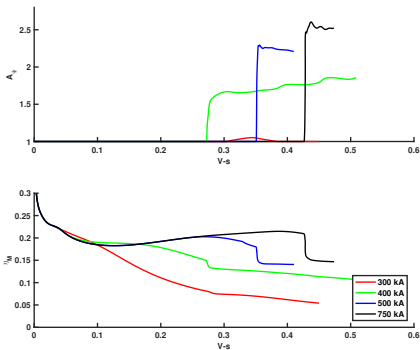
$t = 6.07611 \times 10^{-5}$ s

- The MHD activity lowers the threshold for the column mode.
- The current filaments are undesirable, because they greatly increase the injector voltage requirements without increasing poloidal flux amplification.

The threshold of the the column mode instability and amount of poloidal flux amplification scale with the injected current.

- We've found two effective limits for I_{inj} :
 - Too low \rightarrow unable to drive the column mode instability
 - Too high \rightarrow drive current filamentation of the flux bubble
- Between those limits, the amount of injected energy retained in the plasma as magnetic energy (η_M) also increases with injected current.

$$\eta_M = \int_V \frac{B^2}{2\mu_0} dV \Big/ \int_0^t |I_g V_g| dt$$

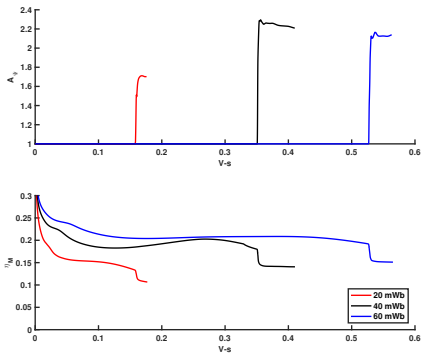


constant $\psi_{bias} = 40$ mWb

When exploring poloidal flux amplification at different values of ψ_{bias} , we scaled the I_{inj} to keep λ_{inj} constant.

- We chose intermediate ramp rates to avoid a diffuse flux bubble and current filamentation.
- The threshold of the column mode and η_M increase with the bias flux and injected current.
- Poloidal flux amplification doesn't strongly scale with the bias flux and injected current.

$$\eta_M = \int_V \frac{B^2}{2\mu_0} dV \Big/ \int_0^t |I_g V_g| dt$$



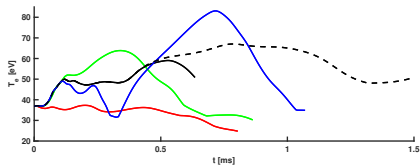
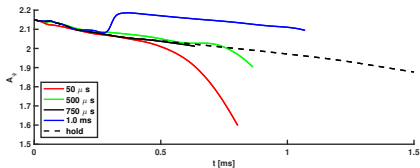
constant $\lambda_{inj} = 5\pi \text{ m}^{-1}$

The highest temperatures in spheromaks are typically observed when the injector current is reduced after the column mode instability.

- The formation of closed flux surfaces is aided by:
 - toroidal current produced by the column mode instability
 - reduction of the injector current, which perturbs the magnetic field
- However, the line-tying of the injector current stabilizes the spheromak to the tilt instability.
- The injector current is also a major contributor to the force balance, so reducing it too quickly degrades confinement.
- We're simulating different injector current traces to explore these competing processes.

Poloidal flux amplification affects spheromak lifetime and peak temperature during decay.

- For the longest decay times, I_{inj} stays above the threshold for current-driven instability long enough to produce additional poloidal flux amplification.
- The highest peak plasma T observed occurs with a decay time of 1.0 ms.
- For even longer decay times than shown, the peak temperature remains low for 100's of μs .
- The peak temperature is maintained for the longest when I_{inj} is reduced and held below the threshold for instability.

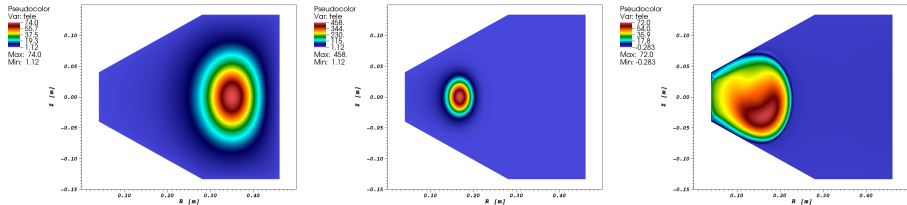


Flux compression

The goal of these calculations is to quantitatively evaluate spheromak performance during magnetic flux compression, in particular compressive heating.

- To achieve fusion temperatures, it's necessary to maintain sufficient thermal confinement during compression.
- Therefore, it's desirable to maintain plasma stability as much as possible during compression.
- For direct comparisons between our 'constructed' equilibrium and compressed states, the computations must start with a stable equilibrium, consistent with the transport model.
- Otherwise, the early evolution will be dominated by the rapid equilibration of the plasma to a new equilibrium state, skewing any comparisons.
- To construct our initial equilibrium, we use series of time-dependent calculations, which requires greater computation expense than direct solution methods, but much less development.

The amount of compressive heating observed in our preliminary flux compression calculations is very encouraging.



- The plasma is compressed with two coils at $R = 60$ cm, $Z = \pm 35$ cm with a linearly ramping coil current.
- With a volumetric compression ratio ~ 8 , the plasma achieves significant amplification of the magnetic field (~ 5) and plasma temperature (~ 6) at the magnetic axis.
- Eventually, the plasma succumbs to an $n_\phi = 6$ instability at $\Delta t \simeq 75 \mu\text{s}$.

Summary & Future Work

Summary

- Computations successfully reproduce the magnetic evolution of multi-pulse shots in SSPX.
- The onset of the column mode (V-s) and poloidal flux amplification are largely insensitive to the injector current ramp rate, which relaxes power supply design requirements.
- Increasing the bias flux significantly increases operational efficiency in terms of the ratio of magnetic-to-injected energy.
- The bias fluxes explored are easily achieved with copper field coils.
- Results suggest that during the multi-pulse sustainment/relaxation phase, the injector current should be held slightly below the threshold for the column mode instability.
- Preliminary results for compression yielded substantial, and encouraging, amounts of plasma heat.

- Continue the formation and decay calculations scanning the injector parameters.
- Explore the effect of the flux conserver and injector geometries on the column mode instability and resulting spheromak performance.
- Continue the flux compression calculations:
 - Determine the sensitivity of compression to the initial equilibrium
 - Determine the optimum rate of compression, which impacts the design requirements of the compression power supply
- Couple the formation and flux compression calculations to simulate an entire discharge from vacuum field through compression.

Acknowledgements

This study uses computational resources from the following facilities:

- The U.S. Army Engineer Research and Development Center (ERDC) DoD Supercomputing Resource Center (DSRC), which is operated by the DoD High Performance Computing Modernization Program (HPCMP).
- The UMBC High Performance Computing Facility (HPCF), which is supported by the US National Science Foundation through the MRI program (grand nos. CNS-0821258 and CNS-1228778) and the SCREMS program (grant no. DMS-0821311), with additional substantial support from the University of Maryland, Baltimore County (UMBC).
- The National Energy Research Scientific Computing Center (NERSC), which is supported by the Office of Science of the US Department of Energy under Contract No DE-AC02-05CH11231.

Access to Sustained Spheromak Physics eXperiment (SSPX) data is provided through the Lawrence Livermore National Laboratory (LLNL). Special thanks to Harry McClean and Bill Meyer for their support.